Site-directed mutagenesis gives insights into substrate specificity of Sulfolobus solfataricus *purine-specific nucleoside hydrolase*

Marina Porcelli, Ester De Leo, Anna Marabotti & Giovanna Cacciapuoti

Annals of Microbiology

ISSN 1590-4261
Volume 62
Number 2

Ann Microbiol (2012) 62:881-887
DOI 10.1007/s13213-011-0379-2

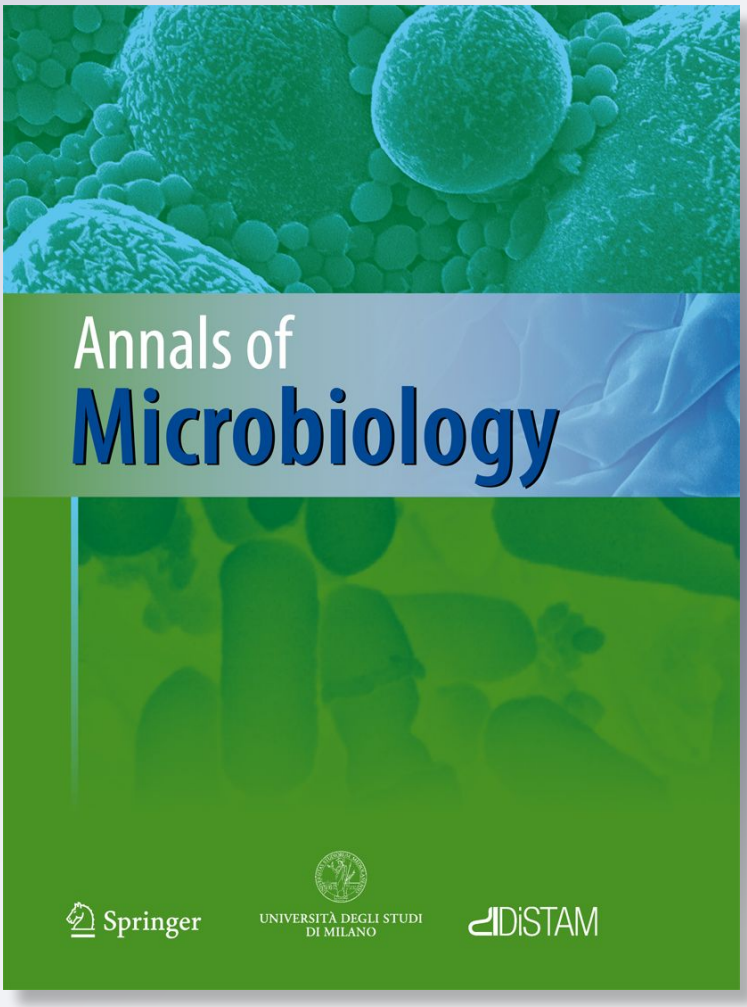

Springer

Ann Microbiol (2012) 62:881–887
DOI 10.1007/s13213-011-0379-2

SHORT COMMUNICATION

Site-directed mutagenesis gives insights into substrate specificity of *Sulfolobus solfataricus* purine-specific nucleoside hydrolase

Marina Porcelli · Ester De Leo · Anna Marabotti · Giovanna Cacciapuoti

Received: 24 May 2011 / Accepted: 19 October 2011 / Published online: 9 November 2011

Abstract Nucleoside hydrolases (NHs) are a class of metalloproteins that catalyze the irreversible hydrolysis of the N-glycosidic bond of β-ribonucleosides forming ribose and purine or pyrimidine base. In the hyperthermophilic archaeon *Sulfolobus solfataricus*, two NHs have been purified and extensively characterized. Although these enzymes show different substrate specificity, one for purines, the other for pyrimidines, their architectures are similar to that of non-specific NHs previously identified in protozoa. The detailed inspection into the active site of the two homologous enzymes obtained by homology modeling allowed us to infer the role of specific residues in substrate specificity. We report here the site-directed mutagenesis of the *Sulfolobus solfataricus* purine-specific inosine-adenosine-guanosine nucleoside hydrolase (SsIAG-NH). The double (L221Y/N228V) mutant of SsIAG-NH was expressed in *E. coli* and purified, and its activity with different substrates was compared to that of the wild-type enzyme. The double substitution modifies the catalytic pattern of the wild-type enzyme affecting both its substrate specificity and catalytic efficiency. Kinetic data obtained for the double mutant are in good agreement with modeling predictions.

Keywords Nucleoside hydrolase · Homology modeling · *Sulfolobus solfataricus* · Site-directed mutagenesis · Substrate specificity

Abbreviations

NH	Nucleoside hydrolase
SsIAG-NH	*Sulfolobus solfataricus* purine-specific inosine-adenosine-guanosine nucleoside hydrolase
SsCU-NH	*Sulfolobus solfataricus* pyrimidine-specific nucleoside hydrolase

Introduction

Nucleoside hydrolases, or nucleoside N-ribohydrolases (NHs) (EC 3.2.2.1), play a key role in the nucleoside salvage pathway by catalyzing, with a hydrolytic mechanism, the cleavage of N-glycosidic bond of β-ribonucleosides with the release of the corresponding free base and ribose (Camici et al. 1990; Versées and Steyaert 2003). NHs are Ca^{2+}-dependent proteins widely distributed in nature, and they have already been found in protozoa, bacteria, yeasts, insects, mesozoa, and plants (Shi et al. 1999; Versées et al. 2001, 2003; Petersen and Møller 2001; Mitterbauer et al. 2002; Ribeiro and Valenzuela 2003; Campos et al. 2005). By contrast, mammals do not contain NH activity (Versées and Steyaert 2003). Based on the substrate specificity of the physiologically relevant form of the enzyme, NHs can be roughly classified into different subclasses: the purine-nonspecific

M. Porcelli (✉) · E. De Leo · G. Cacciapuoti
Dipartimento di Biochimica e Biofisica "F. Cedrangolo", Seconda Università di Napoli,
Via Costantinopoli 16,
80138 Naples, Italy
e-mail: marina.porcelli@unina2.it

A. Marabotti
Istituto di Tecnologie Biomediche del CNR,
via F.lli Cervi 92,
20090 Segrate, (Milano), Italy

A. Marabotti
Istituto di Scienze dell'Alimentazione del CNR,
via Roma 64,
83100 Avellino, Italy

inosine-uridine nucleoside hydrolase, the purine-specific inosine-adenosine-guanosine nucleoside hydrolase, the pyrimidine-specific nucleoside hydrolase, and the 6-oxo-purine-specific inosine-guanosine nucleoside hydrolase (Versées and Steyaert 2003).

The metabolic role of NHs is well established only for parasitic protozoa (Shi et al. 1999; Versées et al. 2001). In these organisms, NHs are key enzymes of the salvage pathway that allow the utilization of purines from their environment. Many NHs from protozoa have been extensively characterized and their crystal structures have been resolved (Shi et al. 1999; Versées et al. 2001; Degano et al. 1996). In addition, these parasitic NHs have been studied extensively in recent years as attractive potential targets for drug development (Schramm 1998).

Diverse and specialized functions have been proposed for NHs (Garau et al. 2010), among them their utilization as pro-drug activators in a novel gene-directed cancer therapy (Giabbai and Degano 2004; Muzzolini et al. 2006). Genomics has led to the identification of several NH sequences, and it is possible that some of these may have useful substrate specificities for the activation of prodrugs.

Very recently, for the first time, two NHs from the hyperthermophilic archaeon *S. solfataricus* have been cloned, expressed, purified, and characterized (Porcelli et al. 2008, 2009). The first one, *Sulfolobus solfataricus* pyrimidine-specific nucleoside hydrolase (SsCU-NH), was identified as a pyrimidine-preferring NH (Porcelli et al. 2008), whereas the second one, SsIAG-NH, shows high specificity for purines (Porcelli et al. 2009). SsIAG-NH shares 43% sequence identity, 66% sequence similarity and the same monomer topology with the homologous pyrimidine-specific SsCU-NH. Despite the different substrate specificities of the two enzymes, a careful evaluation of their sequence and structural features with several alignment methods and predictors for fold recognition allows to classify both as members of the purine-nonspecific inosine-uridine-NH class (Porcelli et al. 2009). In addition, a comparison of the active site of the two enzymes shows that the residues contacting the ribose moiety of the substrate and those coordinating a Ca^{2+} ion necessary for catalysis are conserved in the sequences of all NHs, and are readily superimposable in the structures. Instead, differences are present in the part of the active site contacting the nucleoside base moiety. In particular, by homology modeling, we have demonstrated that in the SsCU-NH active site it is possible to identify bulky residues acting as steric hindrances, thus impairing the positioning of purine nucleosides. These residues are replaced by smaller ones in the SsIAG-NH active site, thus allowing the accommodation of purine nucleosides (Porcelli et al. 2009).

To substantiate this argument, and to shed light on the molecular determinants for substrate specificity of these archaeal enzymes, we have carried out the site-directed mutagenesis of SsIAG-NH, and have analyzed the kinetic properties of mutant recombinant enzyme in comparison with the wild-type, demonstrating the influence of the L221Y/N228V double mutation on the function of the archaeal NH.

Materials and methods

Bacterial strains, plasmid, enzymes and chemicals

Escherichia coli strain BL21(λDE3) was purchased from Novagen (Darmstadt, Germany). Plasmid pET-22b(+) and the NucleoSpin Plasmid kit for plasmid DNA preparation were obtained from Genenco (Duren, Germany). Specifically synthesized oligodeoxyribonucleotides were obtained from MWG-Biotech (Ebersberg, Germany). Restriction endonucleases and DNA-modifying enzymes were obtained from Takara Bio (Otsu, Shiga, Japan). *Pfu* DNA polymerase was purchased from Stratagene (La Jolla, CA, USA). Nucleosides, purine and pyrimidine bases and standard proteins used in molecular mass studies were obtained from Sigma (St. Louis, MO, USA). And isopropyl-βD-thiogalactoside was from Applichem (Darmstadt, Germany). All reagents were of the purest commercial grade.

Mutagenesis of SsIAG-NH, expression and purification

L221Y/N228V mutant of SsIAG-NH was generated by site-directed mutagenesis using the QuickChange kit (Stratagene). The *SsIAG-NH* gene SSO2243 (GenBank™ accession number AE006829.1) cloned into the pET-22b(+) expression vector was used as a template. Primers for site-directed mutagenesis were designed according to the instructions for the QuickChange kit. Mutations were confirmed by DNA sequence analysis. The purified plasmids were used for transformation of *Escherichia coli* BL21 (λDE3) cells. At a late stage of cellular growth, isopropyl-βD-thiogalactoside was added at 1 mM final concentration and the induction was prolonged for 16 h. Cells (10 g) were harvested by centrifugation (15 min, 5,000 *g*, 4°C) and lysed as described by Sambrook et al. (1989). Harvested cells were resuspended in 50 mM Tris/HCl, pH 8 (3 ml/g of wet cells), containing 100 mM NaCl, 135 μM PMSF, and lysozyme (0.25 mg/ml final concentration) and incubated at room temperature for 30 min. Four milligrams of deoxycholic acid per gram of cells were then added under continuous stirring and the mixture was incubated at 37°C. When the lysate became viscous,

DNase (Boehringer) was added to a final concentration of 0.14 mg/ml and the incubation was continued for 1 h at room temperature. The cell debris was removed by centrifugation at 20,000 *g* for 60 min at 4°C and the supernatant was used as a cell-free extract.

All the purification steps were performed at room temperature. Mutant SsIAG-NH was easily purified to homogeneity by a fast and efficient two-step procedure. The first step in the purification of the protein from crude cell lysate was an optimized heat precipitation, made possible by the extreme thermostability of the enzyme. The cell-free extract of BL21 *E. coli* cells expressing mutant SsIAG-NH was heated at 100°C for 10 min and centrifuged at 15,000 *g* for 60 min. After dialysis overnight against 10 mM Tris/HCl pH 7.4, the enzyme was applied to an affinity column of 5′-methylthioinosine-Sepharose (2× 12 cm) prepared as described by Porcelli et al. (2009) and equilibrated with 20 mM Tris/HCl pH 7.4. The column was washed stepwise with 50 ml of the equilibration buffer and then with the same buffer containing 0.5 M NaCl until the absorbance at 280 nm reached the baseline. Nucleoside hydrolase activity was then eluted with 20 mM Tris/HCl pH 7.4 containing 0.5 M NaCl and 3 mM inosine. Active fractions were pooled, concentrated and dialyzed extensively against 10 mM Tris/HCl pH 7.4.

As shown in Fig. 1, which reports the analysis, by SDS-polyacrylamide gel electrophoresis of recombinant mutant SsIAG-NH at different stages of purification, most *E. coli* thermolabile proteins can be denaturated and precipitated by heating, and only minor contaminants of thermostable recombinant mutant SsIAG-NH are detectable. The remaining impurities were removed by an affinity chromatography on 5′-methylthioinosine-Sepharose. About 1 mg of enzyme preparation with a 19% yield was easily obtained from 1 l of colture.

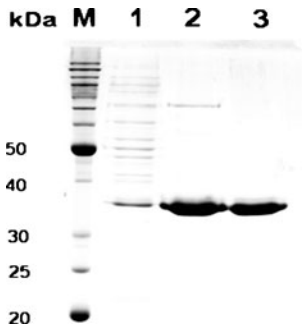

Fig. 1 SDS-polyacrylamide gel electrophoresis of recombinant double mutant SsIAG-NH at different stages of purification. *Lane 1* *E. coli* BL21 transformed with pET-L221Y/N228V-SsIAG-NH crude extract (20 μg); *lane 2* the same sample as *lane 1* heated at 100°C for 10 min and cleared by centrifugation at 15,000 g (10 μg); *lane 3* the same sample as *lane 2* after affinity chromatography (2 μg); *Lane M* molecular mass markers

Several criteria were evaluated to assume the homogeneity of the enzyme. Under denaturating and native conditions, the purified enzyme migrates as a single band on polyacrylamide gel electrophoresis. When assays are carried out on the material eluted from gel slices under native conditions, the activity corresponds to the protein band.

Enzyme assay

NH activity was determined following the formation of purine/pyrimidine base from the corresponding nucleoside by HPLC using a Beckman system Gold apparatus. Unless otherwise stated, the standard incubation mixture contained the following: 10 μmol Tris/HCl buffer, pH 7.4, 200 nmol of the nucleoside and the enzyme in a final volume of 200 μl. The incubation was performed in sealed glass vials for 5 min at 80°C. The vials were rapidly cooled in ice and the reaction was stopped by the addition of 100 μl of 10% trichloroacetic acid. Control experiments in the absence of the enzyme were performed in order to correct for nucleoside hydrolysis. An Ultrasphere ODS RP-18 column was employed and the elution was carried out with 6:94 (v/v) mixture of 95% methanol and 0.1% TFA in H_20. The retention times of adenosine and adenine, inosine and hypoxantine, guanosine and guanine, uridine and uracil, cytidine and cytosine were 12.2 and 6.2 min, 10.5 and 4.7 min, 15.2 and 6.1 min, 6.8 and 4.2 min, and 6.6 and 3.9 min, respectively. The amount of purine or pyrimidine base formed is determined by measuring the percentage of the absorbance integrated peak area of purine or pyrimidine base formed with respect to the total (nucleoside+purine/pyrimidine base) absorbance integrated peak areas. In all othe kinetic and purification studies, the amount of the protein was adjusted so that no more than 10% of the substrate was converted to product and the reaction rate was strictly linear as a function of time and protein concentration. One unit of enzyme activity was defined as the amount of enzyme that catalyzes the cleavage of 1 nmol of nucleoside/min at 80°C.

Determination of kinetic constants

Homogeneous preparations of SsIAG-NH and of the double mutant were used for kinetic analysis. The enzymes gave a linear rate of reaction for at least 10 min at 80°C; thus, an incubation time of 5 min was employed for kinetic experiments. All enzyme reactions were performed in triplicate. Kinetic parameters were determined from Lineweaver–Burk plots of initial velocity data. K_m and V_{max} values were obtained from linear regression analysis of data fitted to the Michaelis–Menten equation. Values given are the average from at least three experiments with

standard errors. The k_{cat} value was calculated by dividing V_{max} by the total enzyme concentration. Calculations of k_{cat} were based on an enzyme molecular mass of 70 kDa.

Protein analysis

Protein concentration was determined by the Bradford method (Bradford 1976) using bovine serum albumin as standard. Protein eluting from the columns during purification was monitored as absorbance at 280 nm. The concentration of SsIAG-NH and of mutant enzyme was estimated spectrophotometrically using ε_{280}=51,910 M^{-1} cm^{-1}. The molecular mass of proteins was determined by gel filtration. The subunit molecular mass was determined by SDS polyacrylamide gel electrophoresis as described by Weber et al. (1972). Protein homogeneity was assessed by SDS-PAGE.

Multiple sequence alignment

Protein similarity searches were performed using the data from Swiss-Prot and Protein Identification Resource (PIR) data banks. The multiple alignment was constructed using the program CLUSTAL W (Thompson et al. 1994).

Molecular modeling

For the structure of SsIAG-NH bound to ligand, the structure of NH from *Crithidia fasciculata* with a transition state inhibitor (PDB code: 2MAS) (Degano et al. 1998) was used as template. The program MODELLER (Sali and Blundell 1993) version 6.1 as implemented in the molecular simulation package InsightII (v.2000.1; Accelrys, 2000) was used to model the monomeric structure of SsIAG-NH in ligand-free and ligand-bound states (Porcelli et al. 2009). The quality of the models and their stereochemical properties were analyzed using the programs PROCHECK (Laskowski et al. 1993) and ProsaII (Sippl 1993).

Results and discussion

In our previous studies (Porcelli et al. 2008, 2009), we analyzed by homology modeling the molecular determinants responsible for different substrate specificity of SsCU-NH and SsIAG-NH. Molecular model analysis reveals that the overall structure and the position of catalytically important residues in the calcium and ribose binding are conserved while the base-binding pocket reflects the difference in substrate specificity between SsCU-NH and SsIAG-NH, strongly supporting the hypothesis that SsIAG-NH and SsCU-NH are homologous enzymes whose active site was partially modified to specifically recognize purine or pyrimidine nucleosides. In Fig. 2 is reported the sequence alignment between SsIAG-NH and SsCU-NH and the amino acid residues, obtained by homology modeling, involved in the corresponding active sites. It seems that the striking different substrate specificity between SsIAG-NH and SsCU-NH could be ascribed mainly to only two differences. The first difference that appears evident is the presence in SsIAG-NH of L221 that replaces Y221 of SsCU-NH. It is interesting to note that this tyrosine residue is a conserved position in *C. fasciculata*-NH where the corresponding Y225 participates in the formation of the catalytic triad required for the protonation of the purine ring (Iovane et al. 2008). The second difference is the presence of N228 of SsIAG-NH that substitutes V228 of SsCU-NH.

It has been proposed that L221 and N228 in SsIAG-NH may play a role in determining enzyme specificity (Porcelli et al. 2008, 2009). Figure 3 reports a close-up

```
                    •  ■•                          ■
SsIAG-NH    MRKVIVDSDTATDDTIAILLASR-FFQLLGVTIVAGNVNYNQEVKNALFTLEYIGKQDVPVYL 62
SsCU-NH     MRHFIIDCDTAEDDVLSLYLLLKNNIDVVAVTIVEGNISYEQEVKNALWALEQVNR-EIPVYP 62
                      ▲  ▲■                                                •
SsIAG-NH    GSQRPILGNWRTVEEVHGSNGMSNWNYPEPNKRPEKEHAIDAILRLSKEHEGELEILAISPLT 125
SsCU-NH     GANKPLLKNYITVEKVHGKGGIGDVTVEPKRLKAQEKHAALAIIDLANEYAGELEFLAISPLT 125
                               ▲        ■▲      ■▲■                        ▲
SsIAG-NH    NIALAYLKDPSVVKRVKKIWIMGG-AFSKGNTTPIAEFNFWVDPEAAKIVLDAGFDITIVPWE 187
SsCU-NH     NLALAYLLDNSIVKKIKKVWVMGGAVFGIGNITPVAEFNIWVDPDAAKIVFNAGFDITMIPWD 187
                                        ▲   ▲    ▲▲       ▲▲•
SsIAG-NH    VAEISGSLNERDWEYISKLNTKLSNFFINVNKTLKEYTTKNQGISGSIHPDSLTVSIAHDNSI 250
SsCU-NH     V-IINYPVTDEEWNVIKNMKTRMSELYVSMYLHYRQYSSTVQKINGHPHPDAITTAIAIDGSI 250

SsIAG-NH    ILDSSLKYVDVELCS-KSRGAMLIDWYSLHK---NKPNAEIVLKADGGKFKNLLFNSLSQL   307
SsCU-NH     ATRREKRFVVIDNTDNITRGMTLVDRFDADTSWSDKPNAEIVYEINKKSFMEKIYDLLNWF   311
```

Fig. 2 Sequence alignment of SsIAG-NH and SsCU-NH. The calcium (●) ribose (■) and base (▲) binding sites are indicated above the alignment. Amino acids modified by site-directed mutagenesis are shown in *white lettering on a black background*. *Numbers on the left* are the coordinates of each protein

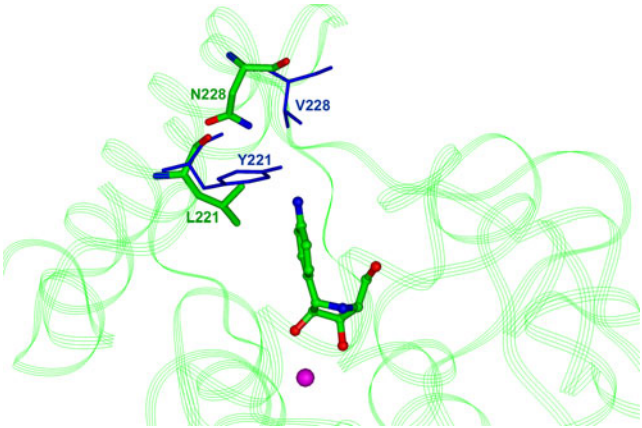

Fig. 3 Close-up of the active site of SsIAG-NH with bound inhibitor (in *ball and stick* mode), calcium ion (the *magenta ball*) and residues L221, N228 represented in *thick stick* mode and color coded: carbon *green*, oxygen *red*, nitrogen *blue*. The backbone of the protein is represented as a *green ribbon*. The equivalent residues Y221 and V228 are superimposed and represented in *thin stick* mode, colored *blue*

of the active site of SsIAG-NH and evidences the different positioning of mutations Y221 and V228 with respect to wild-type residues L221 and N228. As shown, in the double mutant of SsIAG-NH, the phenolic moiety of Y221 is protruding towards the interior of the active site and it is possible to see that this residue is practically in contact with the molecule of the ligand. In contrast, the smaller side chain of Leu in wild-type enzyme is far from it. In addition, the side chain of N228 leaves a bigger cavity in the active site of the enzyme with respect to V228. Therefore, in the double mutant of SsIAG-NH, the presence of these two mutations in the active site could result in a combined effect: the increased steric clashes would impair the binding of bigger purine nucleoside, and the presence of Y221 would favor the interaction with the smaller pyrimidine bases.

In the absence of the three-dimensional structures of the two thermophilic NH from *S. solfataricus*, presently under investigation, to confirm the role of these two amino acid positions in substrate binding, we performed the site-directed mutagenesis of SsIAG-NH generating a double mutant protein L221Y/N228V. The mutant SsIAG-NH gene was overexpressed in *E. coli* and the recombinant protein was purified and assayed for substrate preference.

Expression and purification of the double mutant used the same methods as for the wild-type enzyme (Porcelli et al. 2009). The mutant protein was obtained in yield and homogeneity comparable with the wild-type enzyme and the analysis of its molecular properties did not reveal any significant difference in the dimeric structure or in the physicochemical properties.

To compare the substrate specificity of the mutant and the wild-type protein, we performed a comparative kinetic analysis of the two enzymes. Initial velocity studies carried out with increasing concentrations of nucleosides gave typical Michaelis–Menten kinetics. The K_m and V_{max} values for nucleoside substrates were calculated. Moreover, the relative efficiency of the nucleoside substrates was determined by comparing the respective k_{cat}/K_m ratios, which are the best measure for comparison of the efficiency of product formation and substrate preference. The kinetic parameters of SsIAG-NH and the double mutant protein are reported in Table 1. The analysis of the kinetic parameters of the L221Y/N228V-SsIAG-NH in comparison with the wild-type enzyme revealed an important role for these residues in substrate binding.

It has been demonstrated that SsIAG-NH is characterized by a broad substrate specificity towards purine nucleosides whereas it was completely inactive towards cytidine and recognizes uridine at very high concentration. SsIAG-NH shows higher affinity for adenosine with respect to inosine and guanosine. On the other hand, the corresponding k_{cat} values and the k_{cat}/K_m ratios indicate that the catalytic efficiency of these substrates is comparable (Table 1). The K_m and k_{cat} values for purine determined in the present study are in close agreement with the previously reported value (Porcelli et al. 2009).

Remarkably, the results obtained on the mutant enzyme indicate that the double substitution modifies the catalytic pattern of the wild-type enzyme affecting both its substrate specificity and catalytic efficiency. Compared to the wild-type enzyme, in fact, the k_{cat} values of the mutant enzyme for all purine nucleoside substrates significantly decreased, whereas the K_m was modified to a lesser extent (approximately two-fold). In contrast, the K_m for uridine decreased 10-fold

Table 1 Kinetic parameters for wild-type and double mutant SsIAG-NH

	K_m (μM)	k_{cat} (s^{-1})	k_{cat}/K_m (s^{-1} M^{-1})
SsIAG-NH			
Inosine	330±20	23.00±0.8	6.9×10^4
Guanosine	150±16	29.20±0.9	19.4×10^4
Adenosine	50±8	3.50±0.1	7.0×10^4
Uridine	3,950±500	0.06±0.002	1.5×10
Cytidine	n.d.	n.d.	n.d.
SsIAG-NH mut			
Inosine	650±70	6.30±0.2	0.97×10^4
Guanosine	320±45	6.30±0.2	1.96×10^4
Adenosine	120±15	1.30±0.04	1.08×10^4
Uridine	400±60	0.61±0.02	1.52×10^3
Cytidine	3,540±450	0.30±0.01	0.85×10^2

Activities were determined at 80°C as described in "Materials and methods"

n.d. not detected

inferring an important role for these residues in substrate binding, while the k_{cat} value increased 10-fold resulting in a catalytic efficiency two orders of magnitude higher than the wild-type enzyme.

Finally, the double mutation allows the enzyme to also recognize cytidine which is hydrolytically cleaved with a catalytic efficiency about 20-fold lower than uridine. It is interesting to note, in this respect, that the Km values obtained with the double mutant in the presence of uridine as substate are comparable to those reported for SsCU-NH (Porcelli et al. 2008) whereas the values with cytidine are almost 4-fold higher.

By comparing the kinetic parameters of the mutant with the wild-type enzyme, two conclusions can be drawn. First, the mutant behaves like the wild-type SsIAG-NH with regard to substrate preference (guanosine>adenosine>inosine). Second, the double substitution causes about 990-fold change in substrate specificity relative to wild-type SsIAG-NH. In fact, the double mutant displays 9.9-fold lower efficiency with guanosine and 100-fold higher efficiency with uridine.

Taken together, these results have largely confirmed previous predictions for active site residues of the two *S. solfataricus* NH indicating that the residues selected in this study have a function for pyrimidine binding.

In conclusion, these findings provide valuable information on the elucidation of the relationship between structure and function of NHs. The replacement of a small amino acid with a larger amino acid may be an effective way to enhance the catalytic efficiency of NHs for pyrimidines. Such information should be of value for the rational design of new inhibitors with potential chemotherapeutic activity and for more selective engineering of NH for use in tumor-directed gene therapy based on the activation of nucleoside analogs prodrugs.

Acknowledgments This research was supported by a grant from "Regione Campania" L.R. n.5/2002 and was partially supported by a grant of "Ministero dell'Università e della Ricerca Scientifica" Prin 2007.

References

Bradford MM (1976) A rapid and sensitive method for the quantitation of microgram quantities of protein utilizing the principle of protein-dye binding. Anal Biochem 72:248–254

Camici M, Tozzi MG, Allegrini S, Del Corso A, Sanfilippo O, Daidone MG, De Marco C, Ipata PL (1990) Purine salvage enzyme activities in normal and neoplastic human tissues. Cancer Biochem Biophys 11:201–209

Campos A, Rijo-Johansen MJ, Carneiro MF, Fevereiro P (2005) Purification and characterization of adenosine nucleosidase from *Coffea arabica* young leaves. Phytochemistry 66:147–151

Degano M, Gopaul DN, Scapin G, Schramm VL, Sacchettini JC (1996) Three-dimensional structure of the inosine-uridine nucleoside N-ribohydrolase from *Crithidia fasciculata*. Biochemistry 35:5971–5981

Degano M, Almo SC, Sacchettini JC, Schramm VL (1998) Trypanosomal nucleoside hydrolase. A novel mechanism from the structure with a transition-state inhibitor. Biochemistry 37:6277–6285

Garau G, Muzzolini L, Tornaghi P, Degano M (2010) Active site plasticity revealed from the structure of the enterobacterial N-ribohydrolase RihA bound to a competitive inhibitor. Struct Biol 10:1–14

Giabbai B, Degano M (2004) Crystal structure to 1.7 Å of the *Escherichia coli* pyrimidine nucleoside hydrolase YeiK, a novel candidate for cancer gene therapy. Structure 12:739–749

Iovane E, Giabbai B, Muzzolini L, Matafora V, Fornili A, Minici C, Giannese F, Degano M (2008) Structural basis for substrate specificity in group 1 nucleoside hydrolases. Biochemistry 47:4418–4426

Laskowski RA, MacArthur MW, Moss DS, Thornton JM (1993) PROCHECK: a programme to check the stereochemical quality of protein structures. J Appl Crystallogr 26:283–291

Mitterbauer R, Karl T, Adam G (2002) *Saccharomyces cerevisiae* URH1 (encoding uridine-cytidine N-ribohydrolase): functional complementation by a nucleoside hydrolase from a protozoan parasite and by a mammalian uridine phosphorylase. Appl Environ Microbiol 68:1336–1343

Muzzolini L, Versées W, Tornaghi P, Van Holsbeke E, Steyaert J, Degano M (2006) New insights into the mechanism of nucleoside hydrolases from the crystal structure of the *Escherichia coli* YbeK protein bound to the reaction product. Biochemistry 45:773–782

Petersen C, Møller LB (2001) The RihA, RihB, and RihC ribonucleoside hydrolases of *Escherichia coli*. Substrate specificity, gene expression, and regulation. J Biol Chem 276:884–894

Porcelli M, Concilio L, Peluso I, Marabotti A, Facchiano A, Cacciapuoti G (2008) Pyrimidine-specific ribonucleoside hydrolase from the archaeon *Sulfolobus solfataricus*-Biochemical characterization and homology modeling. FEBS J 275:1900–1914

Porcelli M, Peluso I, Marabotti A, Facchiano A, Cacciapuoti G (2009) Biochemical characterization and homology modeling of a purine-specific ribonucleoside hydrolase from the archaeon *Sulfolobus solfataricus*: Insights into mechanisms of protein stabilization. Arch Biochem Biophys 483:55–65

Ribeiro JM, Valenzuela JG (2003) The salivary purine nucleosidase of the mosquito, *Aedes aegypti*. Insect Biochem Mol Biol 33:13–22

Sali A, Blundell TL (1993) Comparative protein modelling by satisfaction of spatial restraints. J Mol Biol 234:779–815

Sambrook J, Fritsch EF, Maniatis T (1989) Molecular cloning: a laboratory manual. Cold Spring Harbor Laboratory Press, Cold Spring Harbor, NY

Schramm VL (1998) Enzymatic transition states and transition-state analog design. Annu Rev Biochem 67:693–729

Shi W, Schramm VL, Almo SC (1999) Nucleoside hydrolase from *Leishmania major*. Cloning, expression, catalytic properties, transition state inhibitors, and the 2.5 Å crystal structure. J Biol Chem 274:21114–21120

Sippl M (1993) Recognition of errors in three-dimensional structures of proteins. Proteins 17:355–362

Thompson JD, Higgins D, Gibson TJ (1994) CLUSTAL W: improving the sensitivity of progressive multiple sequence alignment through sequence weighting, position-specific gap penalties and weight matrix choice. Nucleic Acids Res 22:4673–4680

Versées W, Steyaert J (2003) Catalysis by nucleoside hydrolases. Curr Opin Struct Biol 13:731–738

Versées W, Decanniere K, Pellé R, Depoorter J, Brosens E, Parkin DW, Steyaert J (2001) Structure and function of a novel purine specific nucleoside hydrolase from *Trypanosoma vivax*. J Mol Biol 307:1363–1379

Versées W, Van Holsbeke E, De Vos S, Decanniere K, Zegers I, Steyaert J (2003) Cloning, preliminary characterization and crystallization of nucleoside hydrolases from *Caenorhabditis elegans* and *Campylobacter jejuni*. Acta Crystallogr D Biol Crystallogr 59:1087–1089

Weber K, Pringle JR, Osborn M (1972) Measurement of molecular weights by electrophoresis on SDS-acrylamide gel. Methods Enzymol 26:3–27